

Summary

Introduction

Rapid environmental change, IPCC, estimated temperature rise.

Trend to precocity in plants, flowering time, etc. Advance in phenology.

Problem: Understanding (and predicting?) long-lived plant adaptation to climate change

Based on previously developed demographic and quantitative genetics model (see), added fluctuating environments. Made theoretical predictions. Estimated fluctuations using data from phenological data (PHENOFIT).

Materials and Methods

Population model

We used a previously developed model with stage-structure (Sandell et al. 2014, master's thesis). We considered to have a population of trees split in two classes, immature (I) and mature (M). The mature individuals are the only one to reproduce. Each year, an immature individual can survive with a probability s_I , mature and reproduce with a probability of m . At the same time, a mature individual has a probability s_M to survive. First-time reproducers, i.e. immature that became mature and reproduce the same year, have a fecundity of f_1 , while experienced reproducers, those who already reproduced at least once, have a fecundity of f_2 . Produced seeds have a probability s_0 to survive and become immature. The standard parameters set is given in (Table 1). The population census is just before reproduction, giving the following Lefkovich matrix (Caswell, 2001):

$$A = \begin{pmatrix} a_{II} & a_{IM} \\ a_{MI} & a_{MM} \end{pmatrix} = \begin{pmatrix} s_0 m f_1 + s_I(1 - m) & s_0 f_2 \\ s_M m & s_M \end{pmatrix} \quad (1)$$

Where a_{ij} describes the contribution of stage j individuals to stage i the next year. With given initial conditions we can compute the number of individuals in the two stages by iterating matrix multiplication by A .

From the original model (Sandell et al. 2014, master's thesis) we implemented density-dependence, so that population will not continuously increase but reach a plateau (see Figure 1). We chose to implement density-dependence through seed germination and survival parameter s_0 using a Beverton-Holt function to avoid chaotic behaviors (Caswell, 2001):

$$s_0 = \frac{s_{0,max}}{1 + k_I N_I + k_M N_M} \quad (2)$$

with k_I and k_M the weights of immature (N_I) and mature (N_M) population respectively. $s_{0,max}$ is the maximum achievable s_0 .

Life-history traits

We considered certain life-history trait s_I , f_1 , f_2 as gaussian for each individual such as:

$$s_I(z) = s_I(\theta_s) \exp\left(-\frac{(z - \theta_s)^2}{2\omega_s}\right) \quad (3)$$

We have similar expressions for f_1 and f_2 . Averaging over the population it gives:

$$\overline{s_I}(\overline{z_I}) = s_I(\theta_s) \sqrt{\frac{\omega_s}{\omega_s + P_I}} \exp\left(-\frac{(\overline{z_I} - \theta_s)^2}{2(\omega_s + P_I)}\right) \quad (4)$$

Again, we obtain similar expressions for $\overline{f_1}$ and $\overline{f_2}$.

Iterations at each time step

Assuming the phenotype has a Gaussian distribution, the mean genotypic value of matures and immatures at the next timestep is given by (Barfield et al. 2011 Eq.5) :

$$\overline{g_I}' = (c_{IM}\overline{g_M} + c_{II}\overline{g_I})(c_{IM}G_M\beta_{a_{IM}} + c_{II}G_I\beta_{a_{II}}) \quad (5a)$$

$$\overline{g_M}' = (c_{MI}\overline{g_I} + c_{MM}\overline{g_M})(c_{MI}G_I\beta_{a_{MI}} + c_{MM}G_M\beta_{a_{MM}}) \quad (5b)$$

With c_{ij} defined as in (Barfield et al., 2011), that is $c_{ij} = \frac{n_j \overline{a_{ij}}}{n_i'}$, it is the contribution of stage j individuals to next years pool of stage i individuals, as a fraction of i individuals at the next time step n_i' ; and $\beta_{a_{II}}$ the gradient of selection as $\beta_{a_{IM}} = \frac{\partial \ln \overline{a_{IM}}}{\partial \overline{z_M}}$.

The first term is a weighted average of mean genotypes contributing to this stage; while the second shows the effect of selection.

A similar recursion is given in (Barfield et al., 2011) for phenotypes. They depend on terms of direct transition from one stage to the other $\overline{t_{ij}}$ and births $\overline{f_{ij}}$ (and we have $\overline{a_{ij}} = \overline{t_{ij}} + \overline{f_{ij}}$):

$$\overline{z_I}' = c_{II}^t(\overline{z_I} + P_I\beta_{t_{II}}) + c_{II}^f(\overline{g_I} + G_I\beta_{f_{II}}) + c_{IM}^f(\overline{g_M} + G_M\beta_{f_{IM}}) \quad (6a)$$

$$\overline{z_M}' = c_{MI}^t(\overline{z_I} + P_I + \beta_{t_{MI}}) + c_{MM}^t(\overline{z_M} + P_M + \beta_{t_{MM}}) \quad (6b)$$

With $\beta_{t_{II}}$ the gradient of selection defined as above in Equation 5a, i.e. $\beta_{t_{II}} = \frac{\partial \ln \overline{t_{II}}}{\partial \overline{z_I}}$; c_{ij}^t the contribution by direct transition of stage j to stage i and c_{ij}^f the contribution by birth.

Approximation under weak selection

Under weak selection, the mean phenotype in the population \overline{z} follow the given approximations under constant environment from (Engen et al., 2011):

$$\overline{z_{eq}} = \frac{\gamma_f \theta_f + \gamma_s \theta_s}{\gamma_f + \gamma_s} \quad (7)$$

With,

$$\gamma_f = \frac{v_I u_I s_0 m \overline{f_1}}{\lambda(P_I + \omega_f)} + \frac{v_I u_M \frac{G_M}{G_I} s_0 \overline{f_2}}{\lambda(P_M + \omega_f)} \quad (8a)$$

and

$$\gamma_s = \frac{v_I u_I \overline{s_I}(1 - m)}{\lambda(P_I + \omega_s)} \quad (8b)$$

γ_f and γ_s represent the respective weight of each of the optimum in the trade-off for $\overline{z_{eq}}$. Indeed, if $\theta_f = \theta_s$ then $\overline{z_{eq}} = \theta_f = \theta_s$. But if $\theta_f \neq \theta_s$, then the trade-off depends on γ_f and γ_s and the ratio between them.

Fluctuating environment

To mimic environmental fluctuations, the optima are fluctuating around a given as such:

$$\begin{cases} \theta_f(t) = \bar{\theta}_f + \alpha_f \xi_f \\ \theta_s(t) = \bar{\theta}_s + \alpha_s \xi_s \end{cases} \quad (9)$$

α_i is the sensitivity of θ_i to noise ξ_i . ξ_f and ξ_s are noise vectors drawn at each time step from a bi-variate normal distribution with respectively σ_f^2 and σ_s^2 variances and correlation ρ_N . Thus we get normal fluctuations, correlated with a correlation coefficient of ρ_N .

Under varying environment, i.e. optima, we get an another approximation under weak selection from (Engen et al., 2011) describing the change of mean phenotype:

$$\Delta \bar{z}(t) = -G_I \gamma (\bar{z}(t) - \theta_v(t)) \quad (10)$$

With

$$\gamma = \gamma_f + \gamma_s \quad (11a)$$

$$\theta_v(t) = \bar{z}_{eq} + \xi_v \quad (11b)$$

$$\xi_v = \frac{\alpha_f \xi_f + \alpha_s \xi_s}{\alpha_f + \alpha_s} \quad (11c)$$

We see that the change in the mean phenotype depends on the sensitivity of the optima as well as on the magnitude of the variations.

Trend in change

To induce a trend in the variation of the optima we use the same formula as above but adding a term depending on time kt :

$$\begin{cases} \theta_i(t) = \bar{\theta}_i + \alpha_i \epsilon(t) \\ \epsilon(t) = kt + \xi_i \end{cases} \quad (12)$$

With k having a negative value, the optima decrease with time.

Phenofit data

PHENOFIT is a phenology model including several models, from environmental and phenological data it simulates populations of trees to predict their range (Morin et al., 2008).

On 6 localities (see Figure 4) we had modeled bud burst date and predicted fitnesses ± 21 days around this date (predicted fitness if bud burst date were modeled date +1 day, -1 day, etc.) from these data we predicted the optima fluctuations. Considering the mean fecundity as a Gaussian function with the same form as f_1 in Equation 4:

$$\beta = \frac{\partial \ln \text{fec}}{\partial \bar{z}} = \frac{\theta_f - \bar{z}}{\omega_f + \sigma_z^2} \quad (13)$$

Using (Lande and Arnold, 1983), with z Gaussian, $p(z)$ the distribution of z in the population, $f(z)$ the fitness associated with z and \bar{f} the mean fitness in the population:

$$\beta = \frac{\text{cov}(z, \frac{f(z)}{\bar{z}})}{\sigma_z^2} \quad (14)$$

From (13) and (14) we can express θ_f :

$$\theta_f = \frac{\text{cov}(z, \frac{f(z)}{\bar{z}})}{\sigma_z^2}(\omega_f + \sigma_z^2) + \bar{z} \quad (15)$$

In our estimations we considered $p(z)$ to be Gaussian around the modeled date by PHENOFIT, with a variance of $P_I = 40$ as in our analytic model. We normalized this distribution so that all dates in the population would be in the 21 days interval around the modeled date.

Trend analyses

All statistical analyses were made using R (R Core Team, 2014), graphics were drawn using ggplot2 (Wickham, 2009), data were handled using dplyr (Wickham and Francois, 2014).

To estimate the trend of the θ_f variations, we considered a trend model with three components: a general decreasing linear trend, a white noise component with a constant variance and a more dramatic noise leading to "catastrophic" events, with negative θ_f values.

Thus to estimate the trend and the regular we wanted to exclude those catastrophic events, thus we kept only value of θ_f over 60, which is lower bound of the realizable range of bud burst date of oak trees. Then we performed a linear regression between values of θ_f and time, giving us an estimation of k from Equation 12. Analyzing the residuals would give us the variance of $\alpha_f \xi_f$ from the same equation.

Results

Constant environment and density-dependence

We used the previously developed model in (Sandell et al. 2014, master's thesis) and simulated (see Figure 1) a tree population for 150 years in constant environment, with and without density-dependence on s_0 , to model a more realistic demography.

Indeed, density-dependence introduced a limit in the population (Figure 1 right panel), as the number of mature and immature individuals seem to converge respectively to 18000 and 10000 individuals, while without density-dependence the population is exponentially growing.

Looking at the phenotype, we started from exactly the same starting point $z = 116$ for phenotypic and genotypic values. Without density-dependence, the population quickly converge to the equilibrium phenotype (\bar{z}_{weak} given by the approximation in Equation 7), $\bar{z}_{weak} = 166$ in this case. With density-dependence the equilibrium is shifted upward ($\bar{z}_{weak,dd} = 121.8$).

This shift is due to the decrease of s_0 in the density-dependent model, indeed because of the initial population $s_{0,dd} = 1.1810^{-3}$ while $s_0 = 0.03$ without density-dependence. This difference, all else being equal, changes the equilibrium of \bar{z}_{weak} . With a lower seed survival, the equilibrium is shifted towards θ_s , i.e. the survival optimum for immature, because it compensates to maintain the demographic equilibrium (growth rate = 1).

Within the density-dependent model the mean immature phenotype \bar{z}_I converge quicker than the mean mature phenotype \bar{z}_M to the equilibrium. It is because of stage-structured nature of our model, the mature stage is a combination of individuals that lived for around 40 generations (given our life-cycle), it buffers adaptation. To change \bar{z}_M , the individual have first to be closer to \bar{z}_{weak} than to survive for a certain number of years and become mature. While the newborns of the given generation are already closer to the equilibrium.

Fluctuating optima

To mimic a more realistic environment we made the optima fluctuate, with various correlations between them. We simulated three populations using the same random seed. We only vary correlations

Parameter	Notation	Value
Life Cycle		
Optimal phenotype for fecundity	θ_f	100
Optimal phenotype for immature survival	θ_s	130
Fecundity function width	ω_f	400
Survival function width	ω_s	400
Heritability	h^2	0.5
Phenotypic variance of immatures	P_I	40
Phenotypic variance of matures	P_M	40
Genotypic variance of immatures	$G_I = P_I \times h^2$	20
Genotypic variance of matures	G_M	20
Survival of immature at phenotypic optimum	$\overline{s_I}(\bar{z} = \theta_s)$	0.8
Fecundity of first time reproducers at optimum	$\overline{f_1}(\bar{z} = \theta_f)$	100
Fecundity of experienced reproducers at optimum	$\overline{f_2}(\bar{z} = \theta_f)$	200
Maturation rate of immature	m	0.02
Combined survival and germination rate of seed	s_0	0.03
Survival of mature stage	s_M	0.99
Density-dependence		
Maximum s_0 in density-dependence function	$s_{0,max}$	0.12
Decreasing factor due to immatures	k_I	0.001
Decreasing factor due to matures	k_M	0.005
Fluctuations		
Sensitivity of optimum for fecundity to fluctuation	α_f	5
Sensitivity of optimum for survival to fluctuation	α_s	5
Noise variance for fecundity	$\sigma_{\xi_f}^2$	3.725
Noise variance for survival	$\sigma_{\xi_s}^2$	3.725
Correlation between noises	ρ_N	0.5
Trend coefficient	k	-0.15

Table 1: Standard parameter set

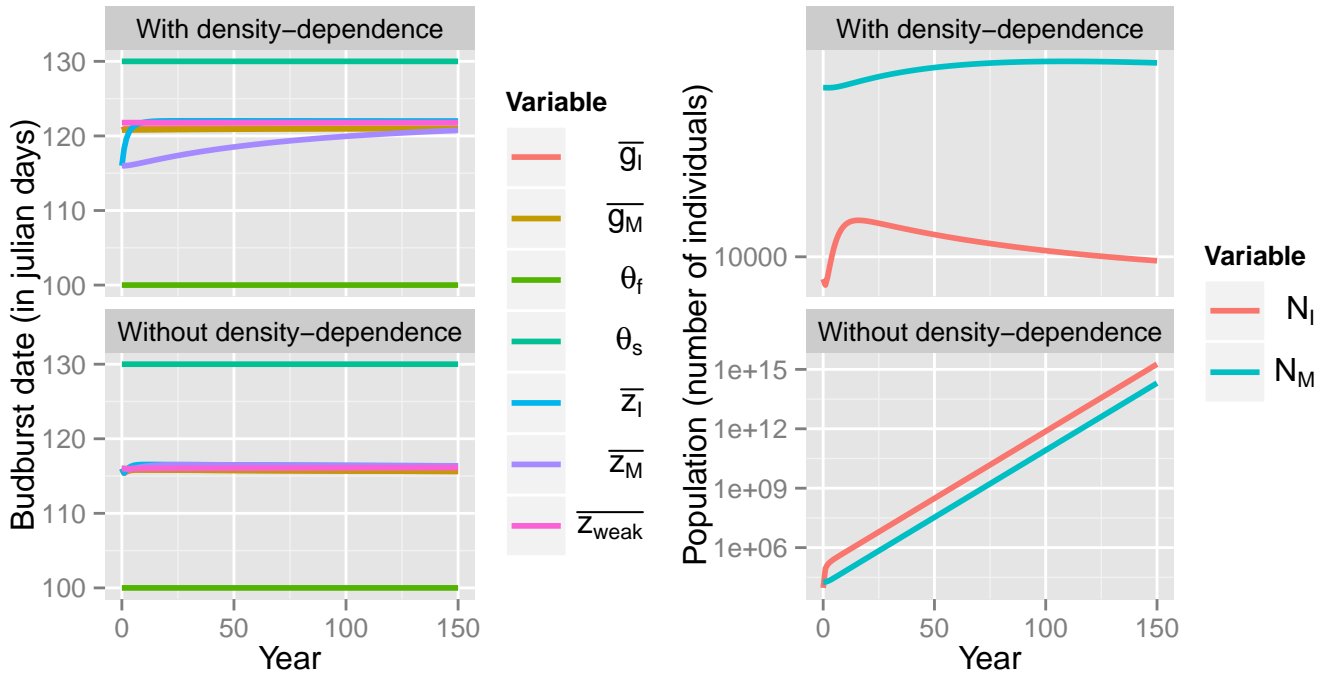


Figure 1: Effect of density-dependence on phenotypes and populations. **Left panel:** Phenotype variations in population (\bar{z}_I, \bar{z}_M) with their corresponding genotypic values (\bar{g}_I, \bar{g}_M) all starting from $z = 166$, and the approximation given by Equation 7; **right panel:** demography, number of immature individuals (N_I , red), number of mature individuals (N_M , blue). Starting from Stable-Stage Distribution (SSD) in constant environment, note the logarithmic scale used.

between noises.

Explain in the text correlation of z_I with $\theta_s(t)$

Trend in the environment

We implemented a decreasing trend in θ_f , linearly and with fluctuations (Figure 3) to mimic climate change. We averaged 15 simulations with fluctuations to understand better the effect of fluctuations.

From Figure 3, as observed in an environment without a decreasing trend, fluctuations make \bar{z}_I fluctuate, while \bar{z}_M not. It is due to the stage-structure of population, indeed the mature class is a buffers variation because it integrates selection over a very long period; while the immature class have new individuals sensitive to current environment each year.

Looking at life-history traits, s_I has an interesting behavior, it first increases, reaches a maximum, than decreases. The decreasing trend in optima variation causes at first the mean population phenotype to move closer to θ_s , thus maximizing s_I values when it crosses θ_s line, as soon as it moves beyond s_I starts to decrease again. The fluctuations seem to decrease s_I (mean difference of 0.5), it may be a cost associated with the variance of optimum fluctuations, the optimum is often under the mean population value.

The fluctuations do not seem to affect fecundity differently from the same environment, f_1 and f_2 decrease because the mean population phenotype go further away from θ_f . Note that they follow exactly the same evolution as the only difference between them is the fecundity value at the optimum date (see Table 1).

Seed germination and survival s_0 is increased by fluctuations, via an indirect mechanism: fluctuations decrease immature survival s_I , thus decreasing the immature population N_I and so the mature population N_M ; this population decrease also decrease competition and density, increasing s_0 as it is density-dependent (see Equation 2).

As expected, the decreasing trend in θ_f creates a lag between the optima and the mean population

values, because adaptation is slower than the rate of change. However, the population can still survive with such a rate if the difference between the optima and the means become constant. On a very long scale (2500 years) it is what happens in this case, the population maintain by changing its phenotype fast enough to track the optima variation (data not shown).

Estimation of the fluctuations

From 6 localities (map [Figure 4](#) bottom left) of PHENOFIT data, we computed θ_f values at these locations (top 3 rows of [Figure 4](#)). For the 6 sites, predicted θ_f decrease with time, it is more precocious as time passes. This observation matches the advance of phenology observed in the literature because of climate change.

Over the general trend, we observe a small amplitude variation around 20 days, corresponding to year to year change in θ_f and some dramatic decreases in its values, sometimes reaching negative values (For example at BIC site in 1976). The frequency of these events increase with time as they become normal after 2050 for all sites. Note that those event are biased towards the decrease of θ_f , as there is no equivalent dramatic increases.

The negative values of θ_f computed in [Figure 4](#), may seem striking as there is no such thing as a negative bud-burst date! However, as bottom right panel of [Figure 4](#) shows, we can have negative value of θ_f and still have achievable phenotypes. And if θ_f is very negative for a given year (less than -100 in 2048 for LAB), it means that will be no reproduction this year.

We excluded those extreme events to estimate the trend in the variation of θ_f (see [Materials and Methods](#)). Using linear regression on θ_f with time, we found a rate of -0.15 d yr^{-1} , with normal residuals having a variance of 93.1 d^2 (data not shown, $R^2 = 0.2435$, $p = 1.185\text{e-}7$, $F = 32.5$ with 101 d.f.).

We investigated to know if there was a break between years modeled from real data by PHENOFIT (before 2001) and years modeled using climate models with climate change included (from 2001). We performed the same regression as above, without taking apart the extreme values, for all sites, splitting the data before 2001 and from 2001. Taking all years, for each site.

Discussion

Difference in \bar{z} and \bar{g} with fluctuations because of selection on viability.

Increasing number of extreme events from predictions.

Authors Contributions and Acknowledgments

References

- Barfield, M., Holt, R. D. and Gomulkiewicz, R. (2011). Evolution in Stage-Structured Populations (2 versions). *The American Naturalist* 177, 397--409.
- Caswell, H. (2001). *Matrix population models : construction, analysis, and interpretation*. Sinauer Associates.
- Engen, S., Lande, R. and Sæther, B.-E. (2011). Evolution of a Plastic Quantitative Trait in an Age-Structured Population in a Fluctuating Environment. *Evolution* 65, 2893--2906.
- Lande, R. and Arnold, S. J. (1983). The Measurement of Selection on Correlated Characters. *Evolution* 37, 1210--1226.

- Morin, X., Viner, D. and Chuine, I. (2008). Tree species range shifts at a continental scale: new predictive insights from a process-based model. *Journal of Ecology* 96, 784--794.
- R Core Team (2014). R: A Language and Environment for Statistical Computing. R Foundation for Statistical Computing Vienna, Austria.
- Wickham, H. (2009). *ggplot2: elegant graphics for data analysis*. Springer New York.
- Wickham, H. and Francois, R. (2014). *dplyr: A Grammar of Data Manipulation*. R package version 0.3.0.2.



Figure 2: Effect of the correlation of fluctuations on phenotypes and life-history traits. Correlation coefficient ρ_N values of noises are indicated at the top of each column. Phenotype and approximations are shown in julian days, \bar{z}_ϵ is the approximation from Equation 10. Mean fecundities are in number of seeds produced. The two bottom rows are survival rates, the top one is \bar{s}_I the mean survival of immature individuals, the bottom one is s_0 the rate of survival and germination of seeds (see Materials and Methods).

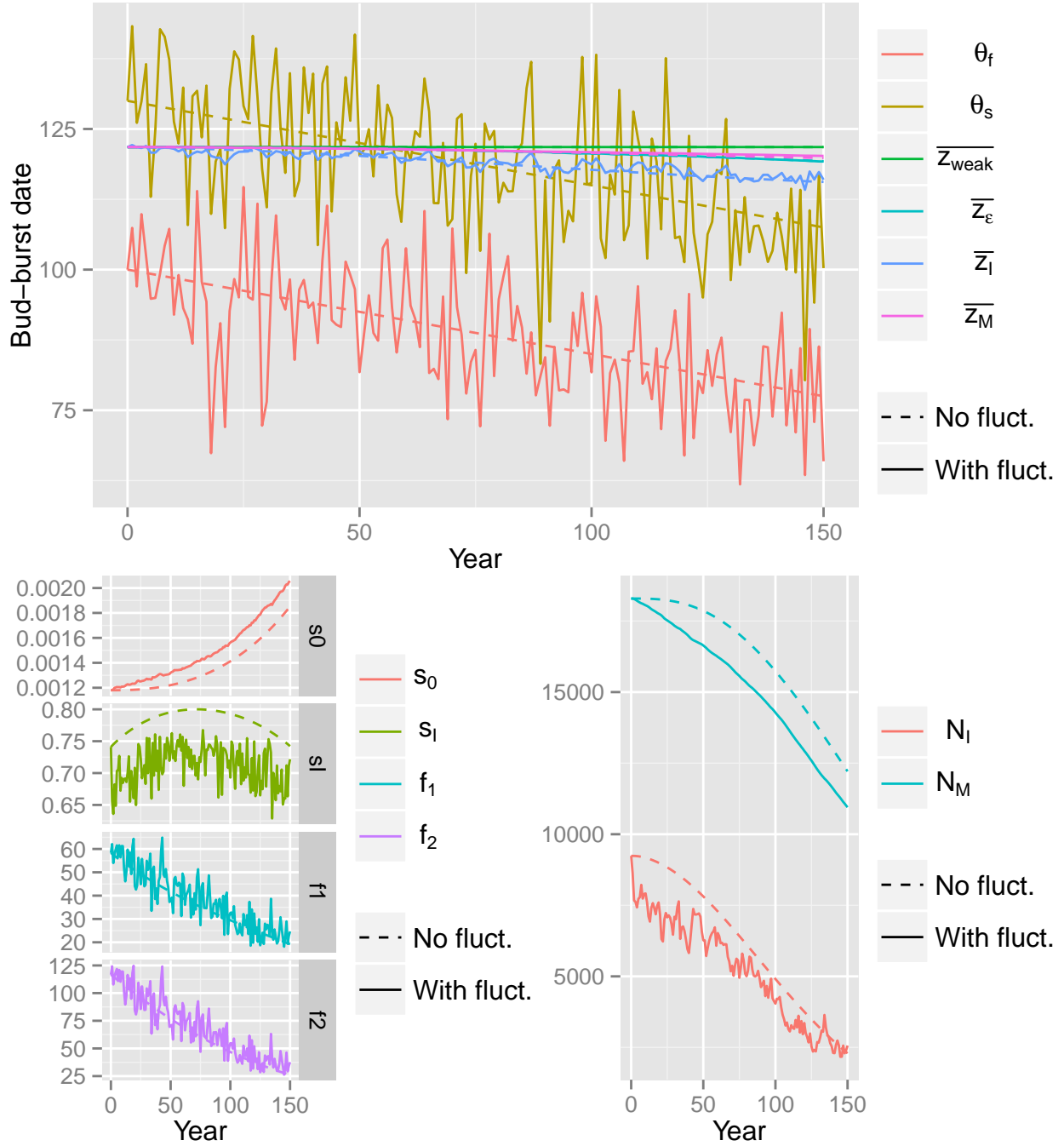


Figure 3: Mixed influences of trend and fluctuations on the population. **Top panel:** Phenotype evolution with and without fluctuations, results from a single simulation; **Bottom panel:** (Left) Life-History Traits evolution depending on fluctuations, survival are rates while fecundities are expressed in produced seeds; (Right) demography. **With fluct.:** fluctuating optima with a linear trend, **No fluct.** linearly decreasing optima. Results shown with fluctuations were averaged over 15 independent simulations for demography and life-history traits.

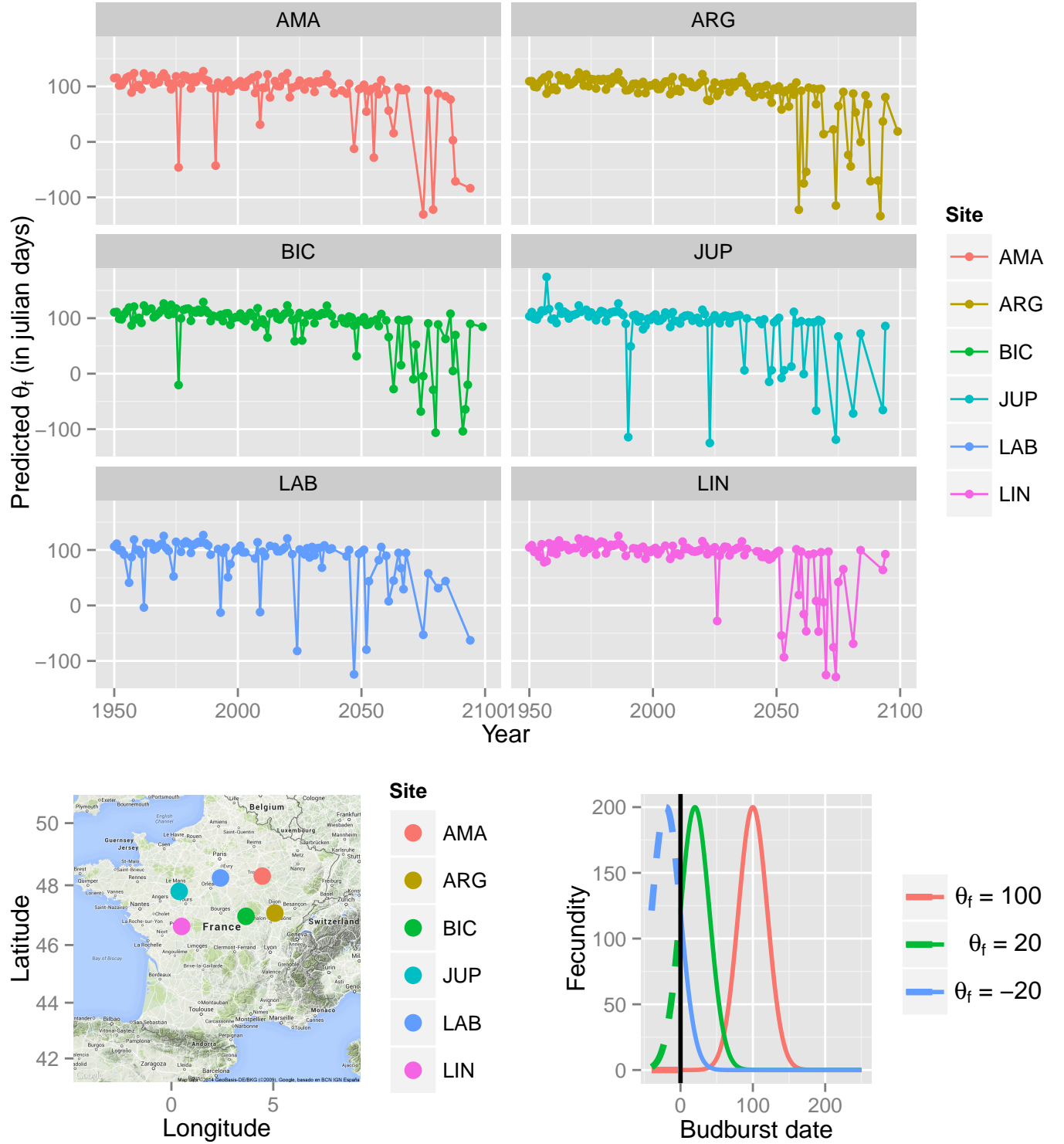


Figure 4: θ_f estimations from PHENOFIT data. Top 3 rows: estimations of θ_f for each study site see [Materials and Methods](#) for details. Bottom left panel: map of the study sites. Bottom right panel: Theoretical fecundity functions with parameters from [Table 1](#) with values of θ_f equals to 100, 20 and -20 , solid lines indicate achievable phenotype, dashed lines show theoretical curves but unreachable phenotypes.